2016-01-01

Evidence Of Active Rifts In The Southwest United States Using Geophysical Inversion Of Seismic Data

Sergio H. Celis
University of Texas at El Paso, shcelis@miners.utep.edu

EVIDENCE OF ACTIVE RIFTS IN THE SOUTHWEST UNITED STATES USING GEOPHYSICAL INVERSION OF SEISMIC DATA

SERGIO CELIS

Master's Program in Geophysics

APPROVED:

Aaron A. Velasco, Ph.D., Chair

Diane I. Doser, Ph.D.

Vladik Kreinovich, Ph.D.

Charles Ambler, Ph.D.
Dean of the Graduate School

EVIDENCE OF ACTIVE RIFTS IN THE SOUTHWEST UNITED STATES USING GEOPHYSICAL INVERSION OF SEISMIC DATA

by

SERGIO CELIS, B.S.

THESIS

Presented to the Faculty of the Graduate School of

The University of Texas at El Paso

in Partial Fulfillment

of the Requirements

for the Degree of

MASTER OF SCIENCE

Department of Geological Sciences

THE UNIVERSITY OF TEXAS AT EL PASO

December 2016

Acknowledgements

I would sincerely like to thank Dr. Aaron A. Velasco, my graduate advisor, for his patience, loyalty, guidance, and commitment to me since my undergraduate studies. I would also like to thank Dr. Diane I. Doser for her guidance throughout my graduate studies and her refusal to accept subpar work. I also would like to thank Cybershare for their funding and commitment to us students during this arduous journey. I would like to thank Lennox Thompson, Ezer Patlan, and Hector Gonzalez for helping me with data processing and always lending a helping hand in whatever I needed. This was truly a collaborative effort, thank you guys. Lastly, I would like to thank my family for supporting me in every aspect throughout this whole process. This experience was as hard on them or even harder than it was on me, thank you for standing by me with unwavering support. This was for you.

Abstract

A continental rift represents a zone where the lithosphere has become thinner due to extensional forces associated with plate tectonics. Many of these rifts are still active, such as the East Africa rift, while others appear to be failed rifts. I build upon recent results of crustal structure for the southern section of the Rio Grande Rift using seismic data collected by USArray stations, and extend the analysis into the states of New Mexico, Oklahoma, Arkansas, and Louisiana to investigate the differences between active and failed rifts in the state of Texas. I collect two geophysical data sets, including receiver functions and surface waves, to perform a joint inversion to determine 1-D S-wave velocity structure. Receiver functions and surface wave dispersion are calculated using Earthscope USArray data from stations in the mentioned states. I use a joint inversion based on constrained optimization that introduces a structural constraint over the inversion model. From the 1-D models, I interpolate layers of the S-wave velocity to create a 3-D velocity model. These results allow me to analyze and locate any possible active or failed rifts in the state of Texas. These results are correlated with geophysical data from the states of New Mexico, Oklahoma, Arkansas, and Louisiana.

Table of Contents

List of Figures

Chapter 1: Introduction

Past geophysical surveys have determined that the state of Texas experienced continental rifting around 1215-1074 Ma in the Central Basin Platform (Adams and Keller, 1993). Other research suggests rifting along the Texas coastline, dating as far back as the late Triassic (Mickus, 2009), when the state of Yucatan and Texas may have been one solid part of the Pangea landmass that was separated by extensive rifting (Mickus, 2009). This study provides new seismological results that will help to better understand the geological past and present of the study region (Figure 2).

Different techniques in computational science and geophysics have been used as quantitative methods to try to understand the internal structure, composition, and dynamics of Earth. Inverse theory is concerned with making inferences about physical systems from data. This investigation presents a joint inversion based on two sets of geophysical data to determine a 1-D S-wave velocity structure, which is based on constrained optimization that introduces a structural constraint over the inversion model. I interpolate between layered 1-D S-wave velocity models to create a 3-D velocity model. This type of model is the primary objective of my geophysical inversion.

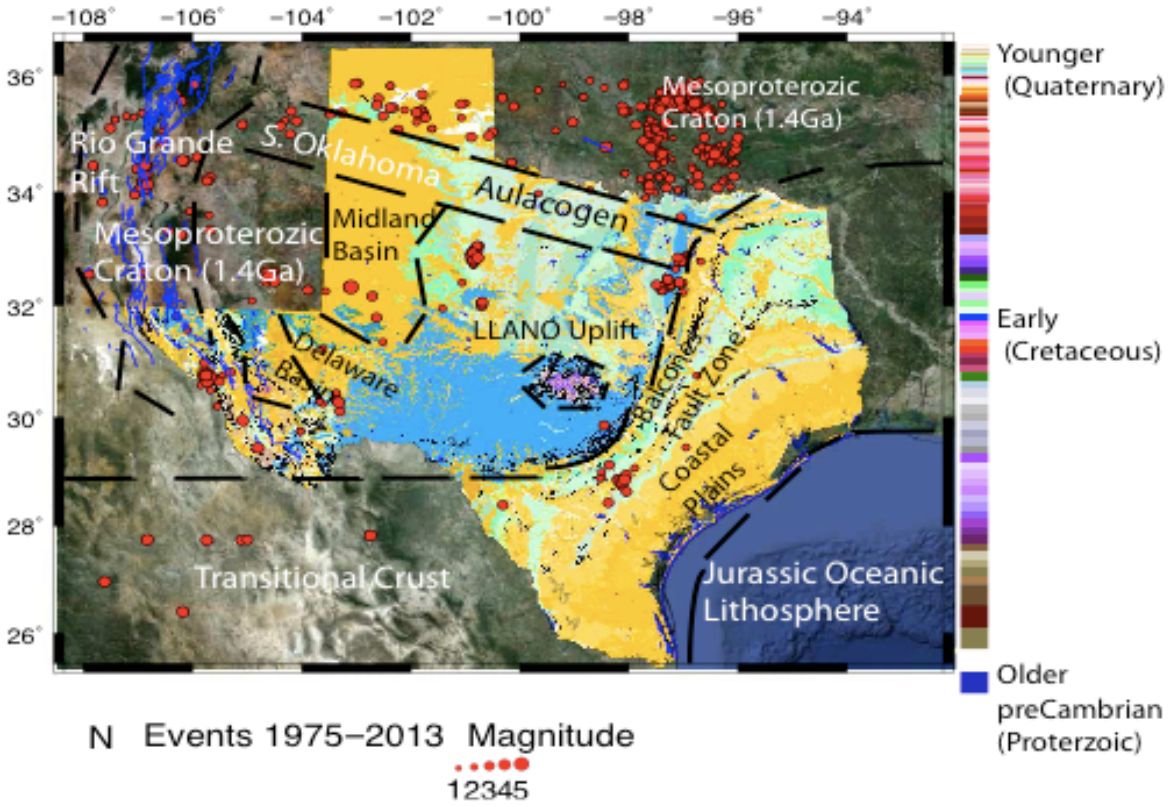

Figure 1.1: Texas map showing geological units along with seismicity of the region over the past 38 years. The map shows the Rio Grande rift region where previous studies were conducted (modified from Thompson 2013).

Chapter 2: Tectonic Setting

The state of Texas covers a total area of 268,581 sq. mi (695,620 km^2). The Texas coastline was part of rift basin and uplift events that occurred in the central part of Texas leading to the eventual separation of the Mexican state of Yucatan and Texas (Mickus, 2009). Texas is mostly composed of sedimentary rocks, with east Texas underlain by a Cretaceous and younger sequence of sediments, the trace of ancient shorelines, until the active continental margin of the Gulf of Mexico is met (Mosher 2008). Magnetic surveys conducted along the Texas coastline show anomalies consistent with other volcanic rift margins like in Namibia (Corner 2002). Previous research shows potential field data for the Texas coast reveals a deeply buried volcanic rifted margin (Adams 1993). This interpretation is consistent with regional sedimentary patterns and detrital zircon ages that indicate the central Texas region was strongly uplifted in Late Triassic time prior to rifting (Mickus and Anthony 2009).

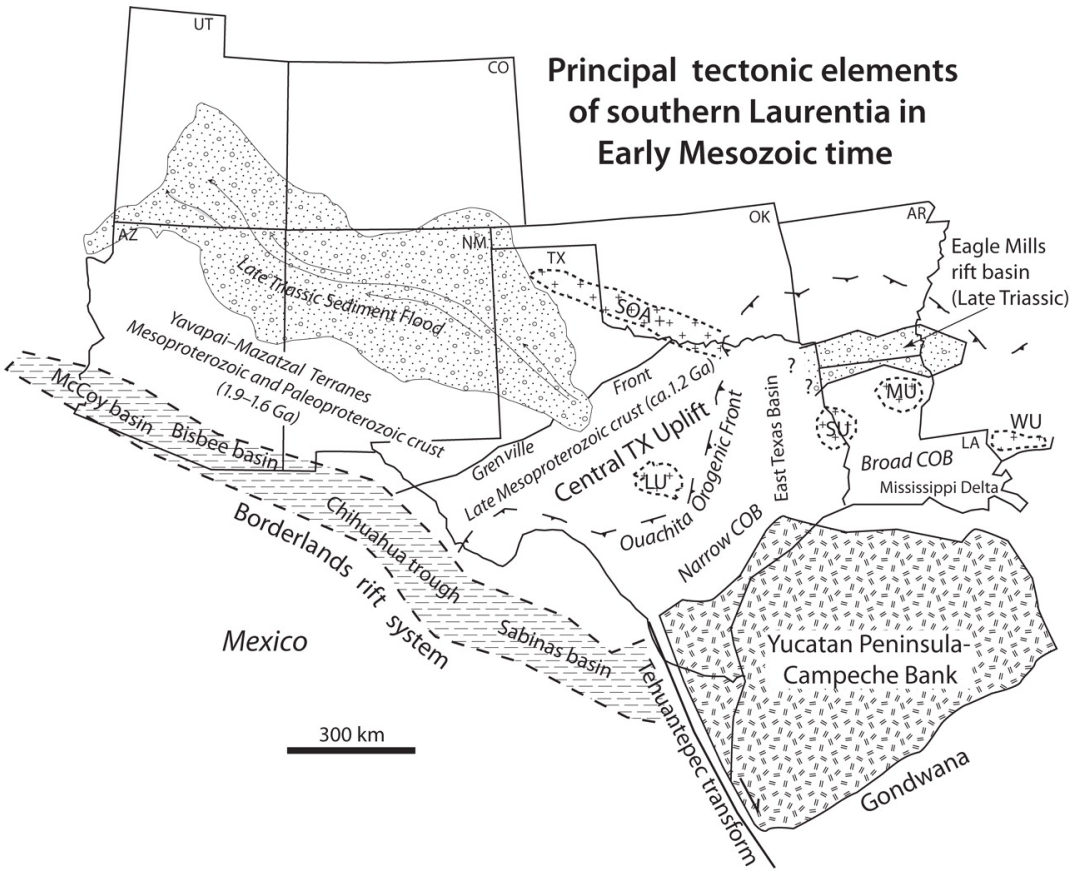

Figure 2.1: Early Mesozoic Map of southwest Laurentia. Buried uplifts: SU-Sabine Uplift, MU-Monroe Uplift, WU-Wiggins uplift. Exposed uplifts: LU-Llano uplift, SOA-Southern Oklahoma uplift (modified from Dickinson and Lawton 2001).

The Central Texas uplift, or Llano uplift (Fig.2), a geologic dome of Precambrian igneous and metamorphic rock, primarily granite, comprises the igneous and metamorphic "heart" of Texas. A ring of gneiss and schist surrounds the region. The Llano uplift was created by continental collision; eventually it became a rifted zone associated with the midcontinent rift system (Lawton and McMillan 1999).

Interpretation of the Texas continent-ocean boundary as a volcanic rifted margin provides a new perspective on the tectonic evolution of the western gulf region. A consensus exists that the NE Mexican margin became a transform continent-ocean boundary (Fig.2), formed by the Jurassic Tehuantepec transform that allowed Yucatan to rotate counterclockwise away from Texas and Louisiana (Pindell, 1985; Dickinson and Lawton, 2001). Rifting of the Yucatan (and Gondwanan fragments to the south) led to the formation of the northwestern Gulf of Mexico basin; this rotation occurred between ca. 160 Ma (Callovian) and 140 Ma (Valanginian) (Bird, 2005). Previous studies infer that a Late Jurassic mantle plume was involved with the opening of the Gulf of Mexico in this region (Bird, 2005).

In the state of New Mexico the Rio Grande Rift (RGR) represents a continental rift formed in the late Oligocene. This rift separates the Proterozoic continental lithospheres of the Western Great Plains and the Colorado Plateau (Keller and Baldridge, 1999).

The northern part of the Texas Panhandle, along with the northwestern part of Oklahoma, is part of a failed rift system called the Southern Oklahoma Rift (SOR). In early Cambrian time, about 540 to 525 million years ago, this area was much like the Red Sea or East Africa.

The state of Oklahoma also experienced rifting during the late Proterozoic. The continent was pulling apart, extending, and the cracks allowed diverse kinds of magmas, from granitic to basaltic, to ascend from deeper in the earth. It pulled apart enough that there was even a general rise in the earth's mantle below what is now southern Oklahoma (Van Schmus and Bickford 1996).

During the early Cambrian, to the northeast of the SOR, another rift was trying to break the continent apart. This is called the Reelfoot Rift or Mississippi Embayment. It runs from northeastern Arkansas and western Tennessee up the Mississippi River to southwestern Indiana

(Figure 2.2). It is possible that both the Southern Oklahoma rift and Reelfoot rift extend into the state of Louisiana.

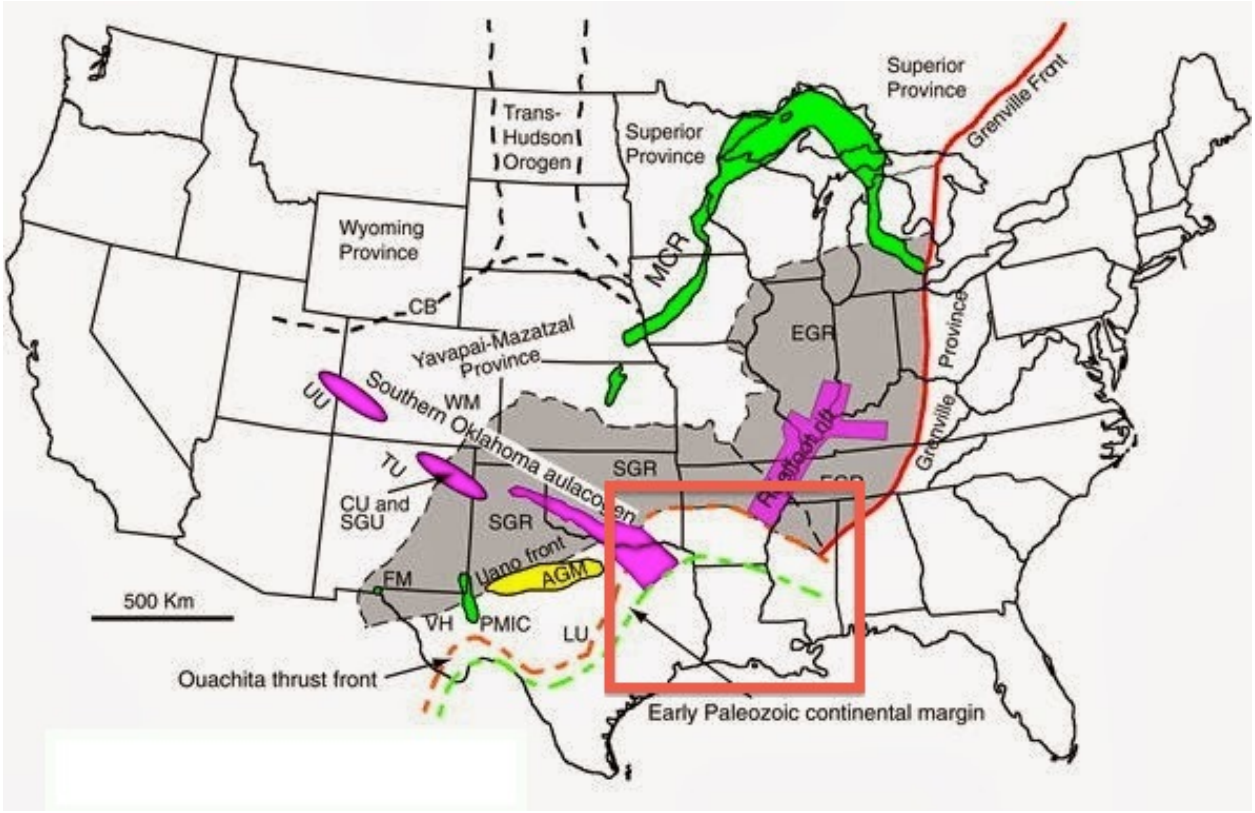

Figure 2.2: Early to Mid-Paleozoic map showing the SOR and Reelfoot rift in purple. Note that both rifts possibly extend into the state of Louisiana shown by the red box (Modified from Van Shmus 1996).

Chapter 3: Data

EarthScope, a program of the National Science Foundation (NSF), deploys thousands of seismic, GPS, and other geophysical instruments to study the structure and evolution of the North American continent and the processes that cause earthquakes and volcanic eruptions. It involves collaboration between scientists, educators, policy makers, and the public to learn about and utilize exciting scientific discoveries. The USArray component of EarthScope offers a continental-scale seismic observatory designed to provide a foundation for integrated studies of continental lithosphere and deep Earth structure. Over the wide frequency range of seismic waves transmitted through the Earth (hundreds of seconds to ten cycles per second), the sensors of the permanent and transportable seismic and magnetotelluric arrays can resolve the smallest background motions at the quietest of sites, while remaining "on scale" for all but the largest ground motions from regional earthquakes (Earthscope 2009).

The primary source of data for this research is obtained from one of the four components that make up the USArray. USArray consists of a portable array (the Transportable Array) of 400 seismometers that have been deployed across the United States over a 10-year period. In addition a "flexible component" array is deployed in areas requiring a denser network of seismometers.

The seismograms used for this study include teleseismic events that were recorded in 2009, 2010, 2011, and 2012. The data were requested through a computer program called Standing Order Data (SOD). The SOD recipe used to request these particular data required the events to be teleseismic, magnitudes of 5.5 or greater, and all were from stations between 25N to 37N latitude and 110 W to 91W longitude. Below are images of TA station locations and corresponding dates.

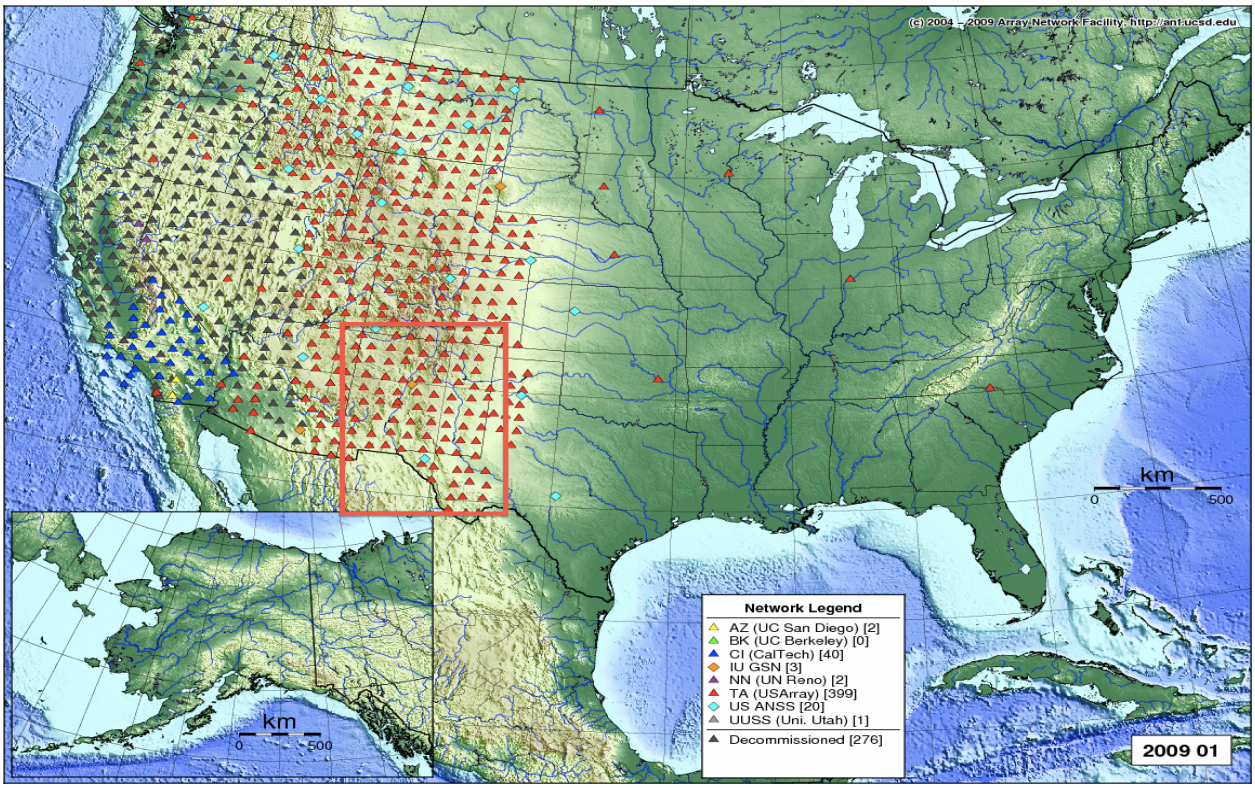

Figure 3.1: Red triangles mark Transportable Array station positions as of Jan 2009. The red rectangle shows the regions of New Mexico and the western part of Texas.

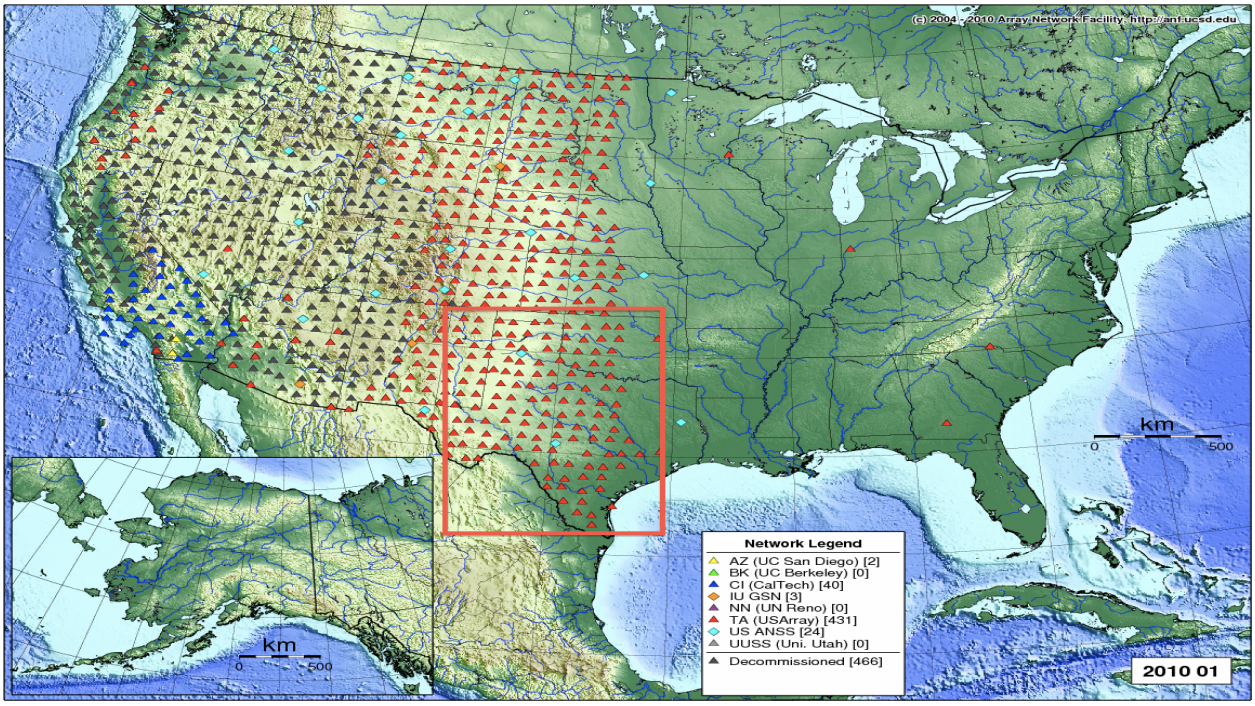

Figure 3.2: Red triangles mark Transportable Array station positions as of Jan 2010. The red rectangle shows the regions of Central Texas and Oklahoma.

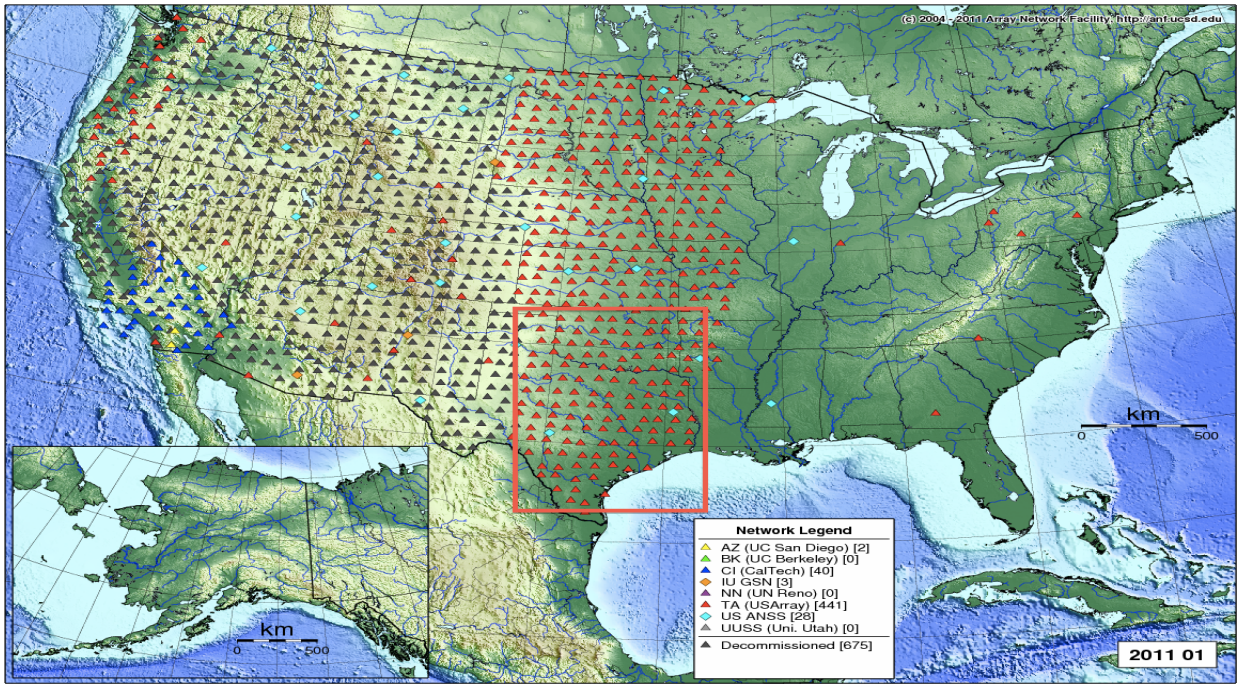

Figure 3.3: Red triangles mark Transportable Array station Positions as of Jan 2012. The red rectangle shows the regions of Eastern Texas and Eastern Oklahoma.

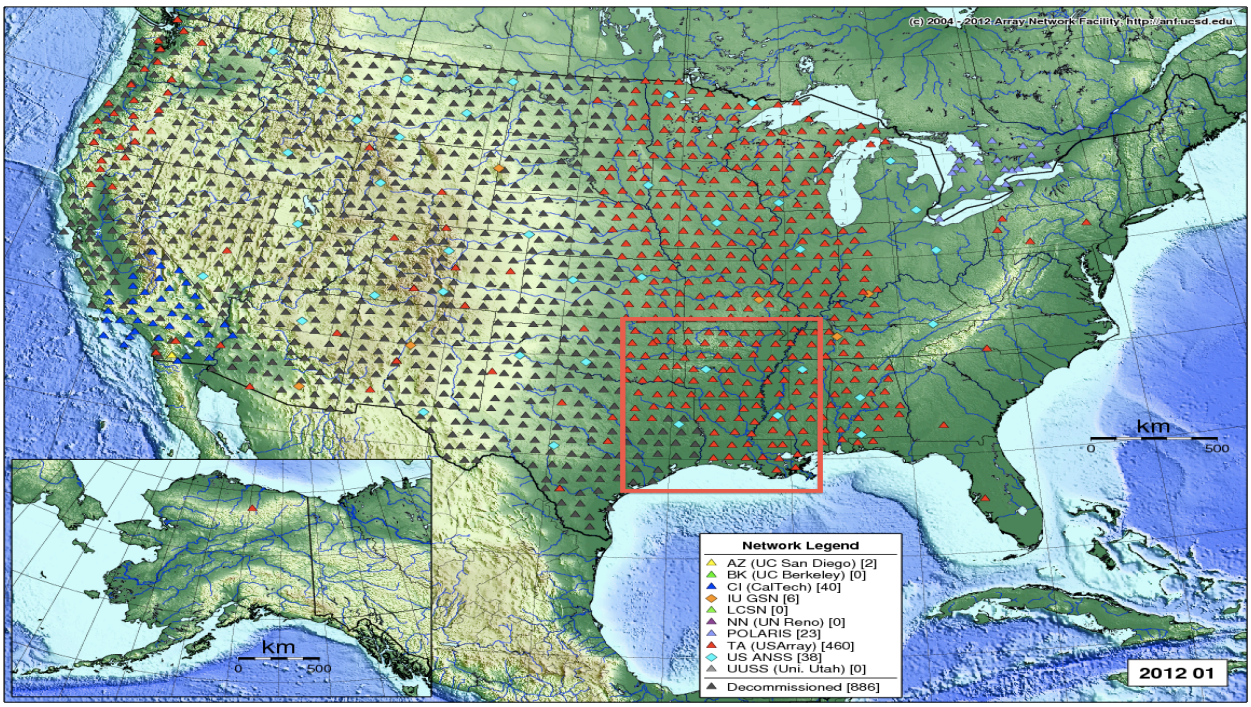

Figure 3.4: Red triangles mark Transportable Array station Positions as of Jan 2012. The red rectangle shows the regions of Arkansas and Louisiana.

Chapter 4: Geophysical Datasets

4.1 RECEIVER FUNCTIONS

A receiver function maps the seismic response of the earth beneath a seismic station for an incoming P-wave. Receiver functions represent a deconvolution of the vertical component of a teleseismic earthquake seismogram from the radial component. The resulting receiver function allows for the identification of converted phases derived from strong impedance contrasts. Receiver functions can provide valuable information for investigating magma lenses within the crust, mantle discontinuities, and rifting extension (Dugda 2005). This receiver function is mainly used to determine the depth of the Moho layer below seismic stations (Ammon 1991). Receiver functions provide an accurate measurement of depth velocity discontinuities and crustal thickness. The time domain iterative deconvolution technique is used in this particular study. The receiver functions show major negative or positive spike amplitudes that correspond to velocity changes. Time separation between phases is used to estimate crustal thickness H from the average crustal velocities (Zhu and Kanamori 2000).

$$H = \frac{t_{Ps}}{\sqrt{\frac{1}{V_s^2} - p^2} - \sqrt{\frac{1}{V_p^2} - p^2}},$$

H is the crustal thickness, t p_s is the time separation between *Ps and P* phases, p is the ray parameter and v_p and v_s are compressional and shear waves respectively. H does not depend as strong on v_p as on v_s, therefore receiver functions show more sensitivity to shear wave velocity contrasts. I use receiver function data sets provided by (Sosa et al., 2013), which includes 485 receiver functions stacked in ray parameter bins based on a receiver function stacking technique

introduced by Zhu and Kanamori (2000), which estimates the crustal thickness and a Vp/Vs ratio based on the radial receiver function.

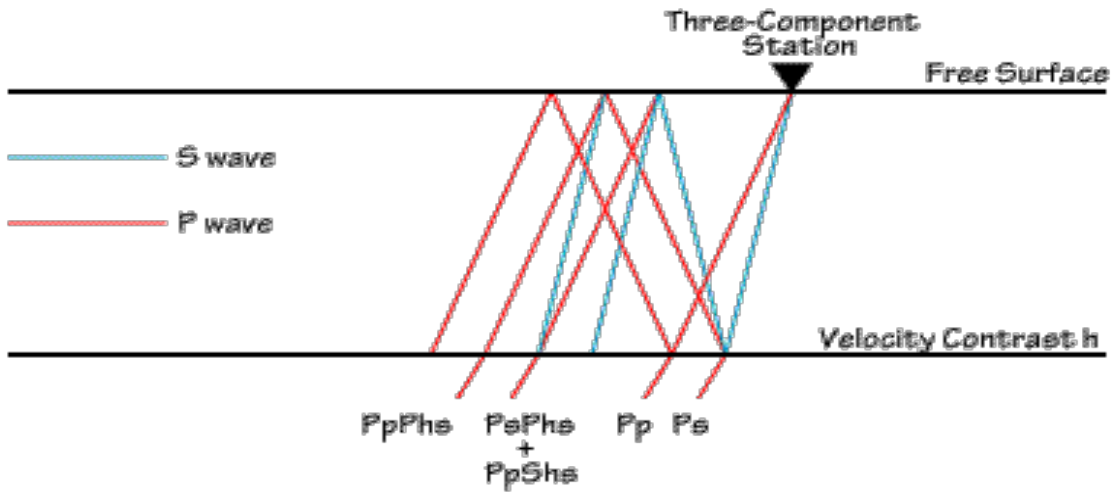

Figure 4.1: Teleseismic P wave corresponding ray paths. With the exception of the first arrival, lowercase letters denote upgoing travel paths (modified from Ammon 1991).

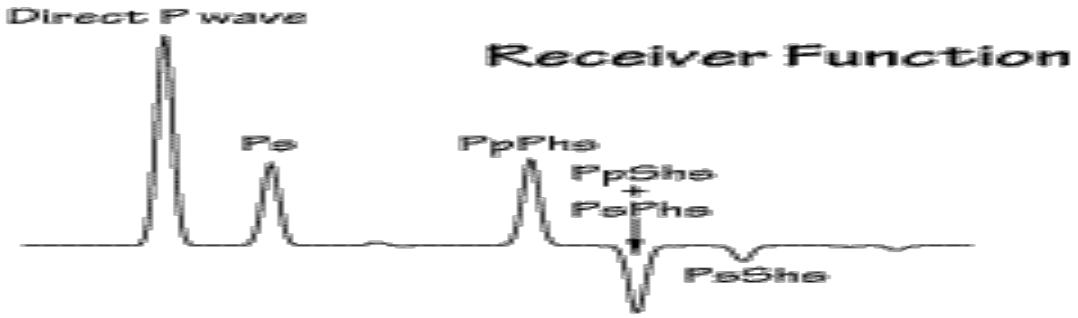

Figure 4.2: Waveform of a Receiver Function, "h" generally represents the depth of the Moho (modified from Ammon 1991).

4.2 SURFACE WAVES

Surface waves dominate seismograms as the largest amplitude waves with lower frequencies than those of body waves. Surface waves become dispersive with velocities that vary depending on the depth range sampled by each period. This study uses periods that range from 10, 50, 100 and 140 seconds (Sosa et al., 2013). Measurements at shorter periods (less than 15 s) show more sensitivity to shallow earth structure including the upper mantle and crust (Herrman et al., 2013). The longer periods provide valuable information for analyzing Earth's deep structure. These velocities provide the data set for one type of source inversion (Liu and Miller, 2011). Dispersion data for the region of interest is obtained from http://www.eas.slu.edu/eqc/eqc_research/NATOMO/distribution.html. Dispersion curves are extracted from three component seismograms recorded at the same station, which correspond to different frequencies and distances using spectral analysis techniques (Maceira and Ammon 2009). Rayleigh's principle states surface wave velocities show more sensitivity to S-wave velocity, although they are theoretically also sensitive to P-wave velocity and density (Julia and Ammon, 2000). The relative contribution of P-wave velocity and density to dispersion is shown to be smaller than that for S-wave velocity.

Chapter 5: Methodology

5.1 JOINT INVERSION

Joint inversion in geophysics represents the simultaneous optimization of several objective functions that allows for estimating a model that interprets all data sets at once (Moorkamp 2010). Joint inversion of multiple data sets does not represent a new concept; most cases using different approaches assume the data sets used in the inversion have similar geological boundaries. Joint inversion can be successful if the following conditions hold: each data set has to sample the same propagating medium and the combination of these data sets increases the resolution of the inverted model (Sosa et al., 2012). The success of our joint inversion relies on the complementarity of the data sets, which imposes physical constraints and thus increases the resolution of the final model. Difficulties arise for highly nonlinear misfit functions and large –dimensional model spaces. Difficulties addressed include the presence of spurious solutions, which are not geophysically meaningful, and the necessity of an appropriate choice of regularization and smoothing constraints. I assume a typical uncertainty value σ_i^2 of .05 km/s for surface waves and .01 for receiver function observations (Julia et al., 2000).

I implement a constrained optimization approach to the joint inversion algorithm and apply the algorithm to the two geophysical data sets in order to find a mutually consistent estimate of a one-dimensional (1-D) Earth structure (Ammon, 2000). Figure 5.1 shows one data set and a joint inversion with two data sets (Sosa et al., 2013).

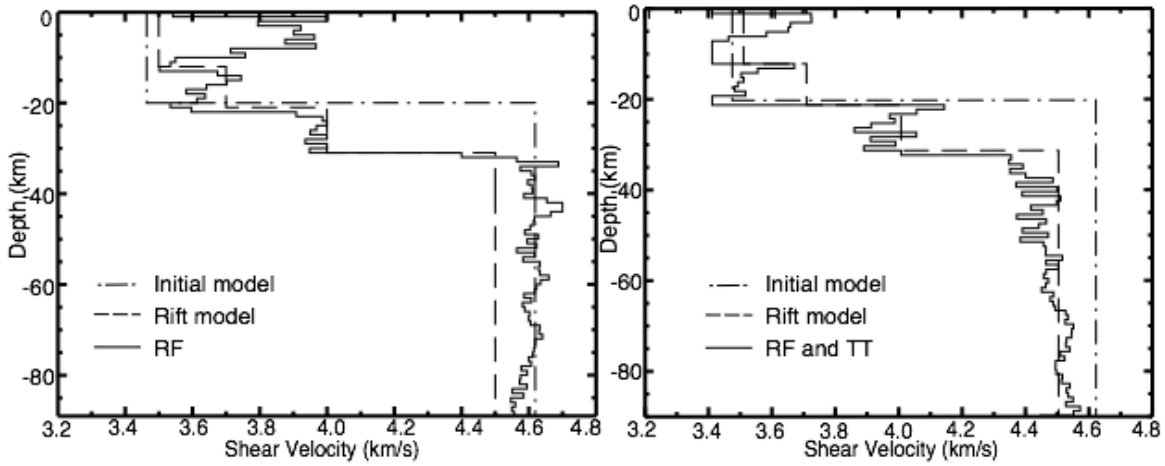

Figure 5.1: Figure shows single inversion of Receiver Functions (left) compared to Receiver Functions (RF) and Travel Times (TT) joint inversion (right). The model on the right is being better resolved by the joint inversion (Sosa et al 2013).

The goal behind the constrained joint inversion approach is to introduce a structural constraint over the model, and provide powerful algorithms for solving large-scale problems. I use the Primal Dual Interior Point Method (PDIP), which belongs to a certain class of algorithms, to solve the linearized version of the inverse problem (Sosa et al., 2013).

Chapter 6: 3D Models and Kriging Results

The primary goal of this study consists of creating a 3-D earth structure of the southwest United States, more specifically Texas, New Mexico, Oklahoma, Louisiana, and Arkansas. For my joint inversion approach I combine the 1-D inverted models with a Bayesian kriging interpolation scheme. The kriging scheme combines the 1-D velocity profiles associated with the transportable US Array stations deployed in the state of Texas during 2010, 2011, and 2012. The interpolated results allow me to estimate 3-D velocity models of the crust and upper mantle for the state of Texas. Interpolation algorithms aim at estimating values of certain quantities by using a weighted sum of surrounding data values. Kriging represents an example of a computationally efficient interpolation technique that allows for incorporating uncertainty into the predicted values (Schultz et al., 1998). Blending the profiles by means of the kriging interpolation scheme can help me provide a better image and interpretation of Earth's structure beneath Texas. I define the crustal and upper mantle structure of the state of Texas using the collected data sets and at the same time provide a different interpretation of some anomalies. The image below shows results of a study done over the Rio Grande Rift in the state of New Mexico. Figure 6.1 is an example of a 3D image from a previous study.

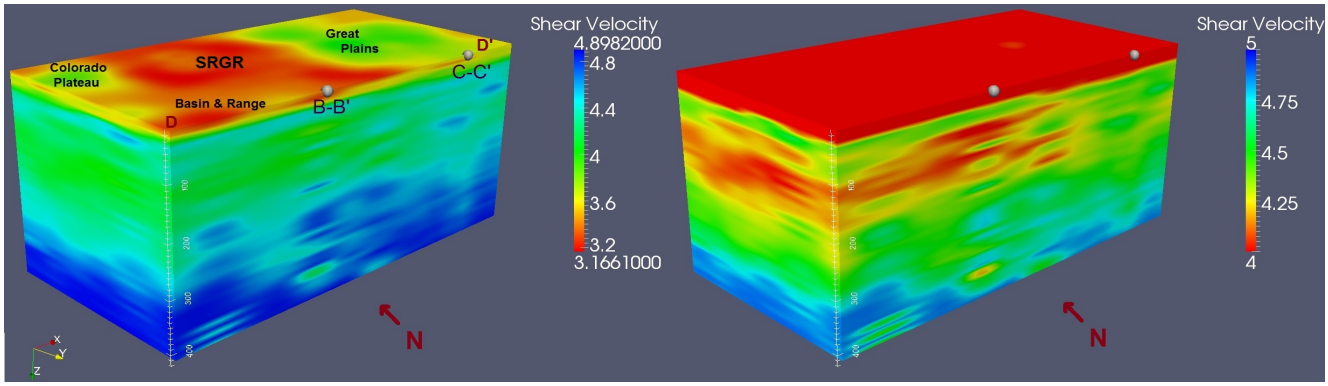

Figure 6.1: 3D Wave Velocity Model. Warmer colors indicate slower S-wave velocities along the Rio Grande Rift (Sosa et al., 2014).

Chapter 7: Results

I have gathered processed seismograms using SOD for the years 2009, 2010, 2011, and 2012. I have run scripts to compute receiver functions for events from 2009-2012. Two difficulties were encountered in the work to date: 1: Several stations had little data, 2: the number of active stations decreases throughout the study period due to their relocation. Data collection is time consuming and difficult since I am searching for events of a fairly high magnitude (5.5 or greater) and they must occur at teleseismic distances. I run c -shell scripts to perform a least-squares (LSQ) joint inversion approach using receiver functions and surface wave dispersions and obtain 1-D velocity profiles as outputs. A constrained optimization approach is applied using Primal Dual Interior Point methods as a solver (Sosa et al., 2013). I then use a matlab script to calculate shear wave velocities (Vs) at depths that range from 10km to 420km below the earth's surface in increments of 10 kilometers. The 1-D velocity profiles are input data for the Bayesian kriging interpolation algorithm used to create the 3-D velocity models (Shultz et al., 1999). The kriging is run on a matlab script. The outputs of the kriging scheme are .dat files that are used to create depth files plotted on GMT to produce cross-section images at different latitudes in our study region. The 3-D models are created in ParaView, an open-source, multi-platform visualization application (Sosa et al., 2014). Figure 11 shows results at approximately 20 kilometers deep Single station "bullseye" indicate heavy sedimentary deposits in that region. The initial velocity model corresponds to the AK-135 model of (Kennett et al., 1995).

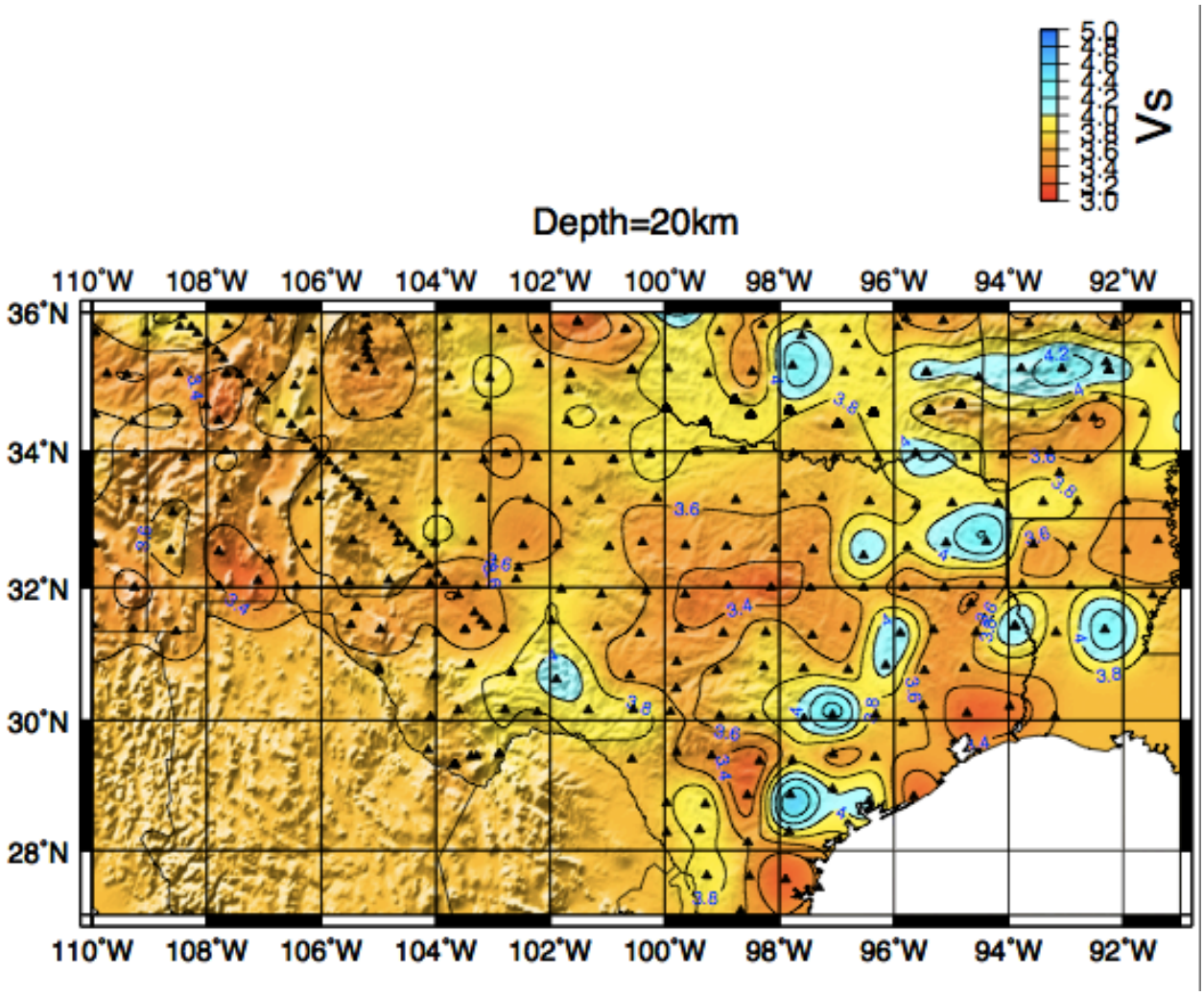

Figure 7.1: Depth slice at 20 km showing shear wave velocity, approximately at the Brittle-Ductile Transition Zone. Black triangles represent array stations including the La Ristra stations trending from NW-SE shown as reference.

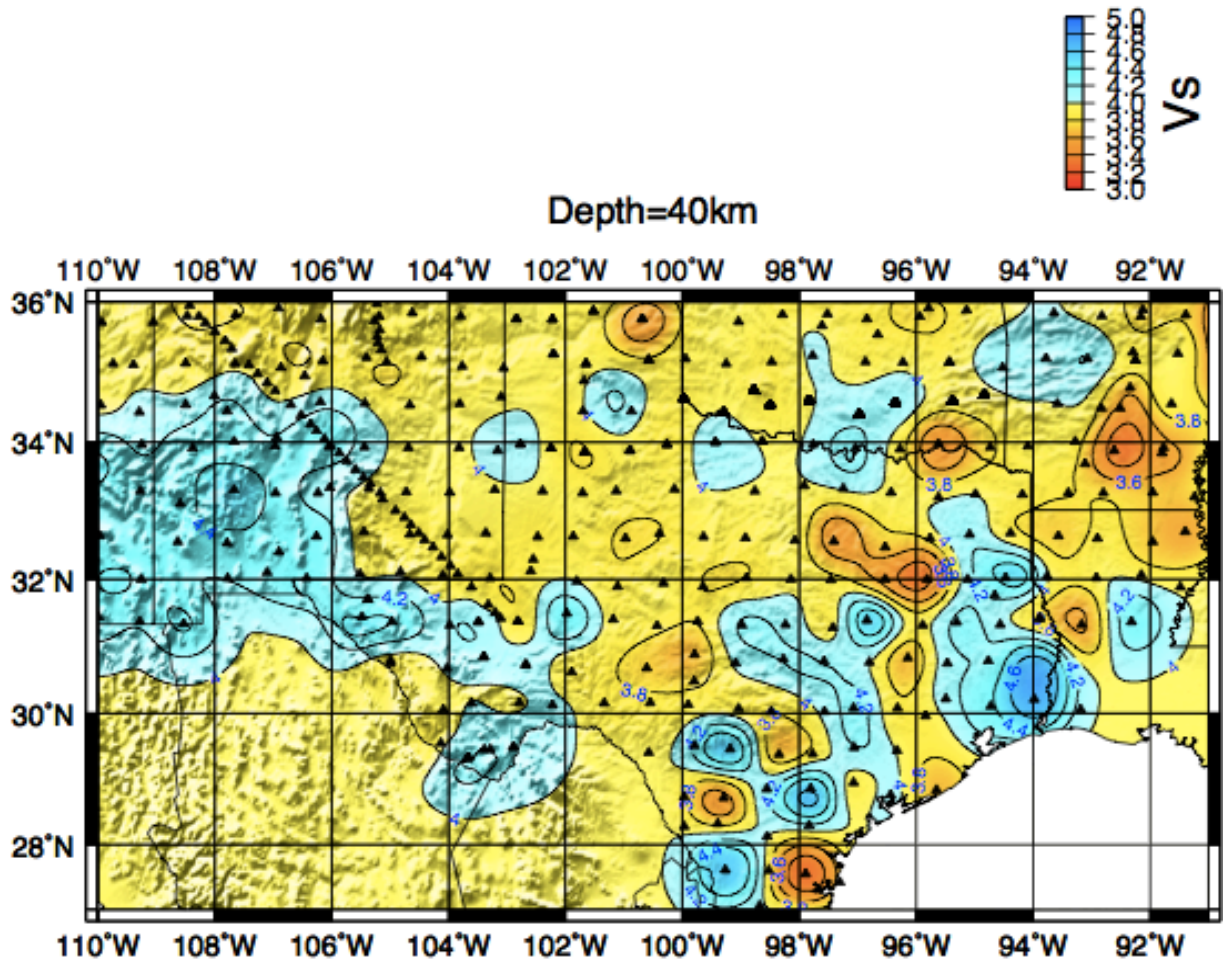

Figure 7.2: Depth slice at 40km showing shear wave velocity near the Moho.

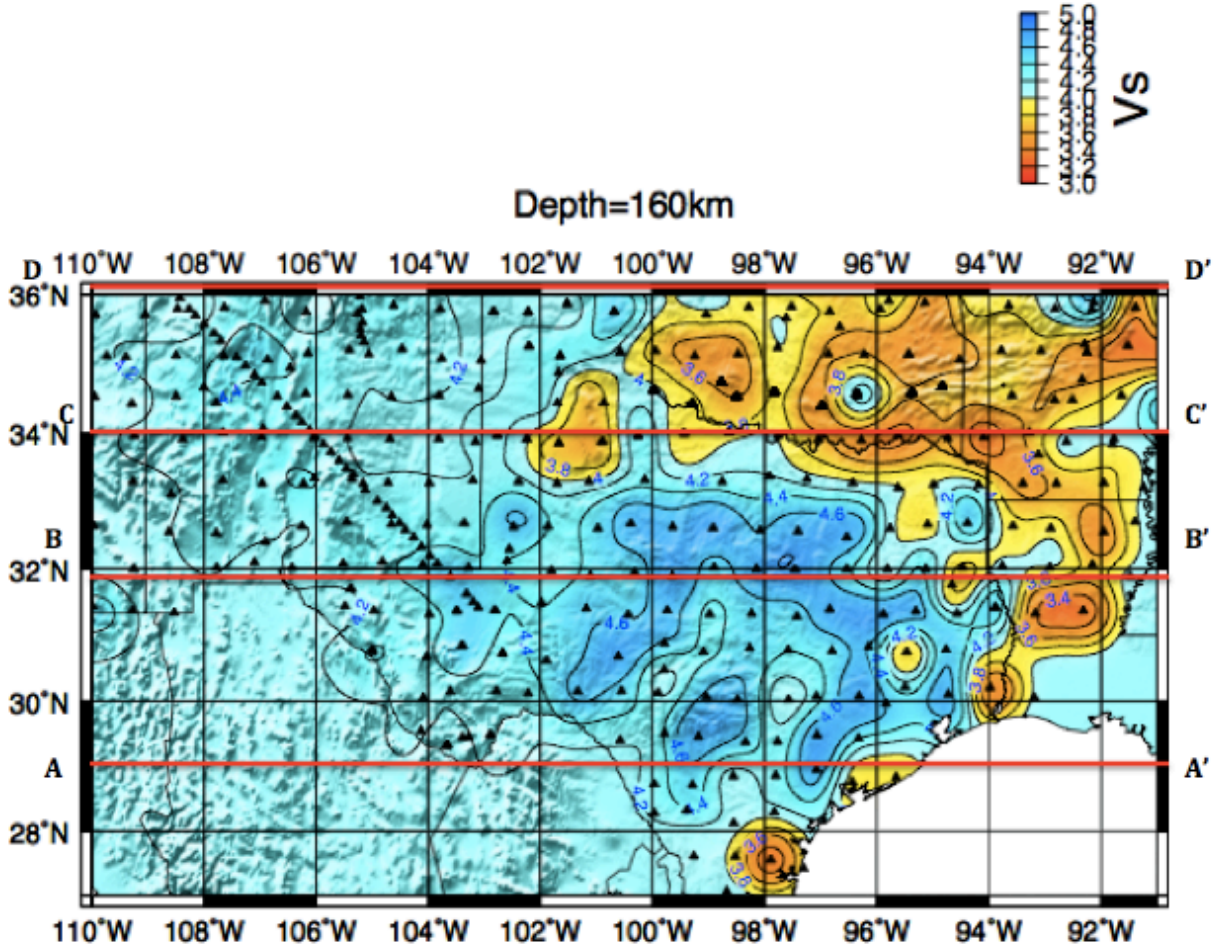

Figure 7.3: Depth slice at 160km showing shear wave velocity at approximately the Lithosphere-Asthenosphere boundary (LAB). A-A' denotes figure 14 cross section at 29 ° N. B-B' denotes figure 15 cross section at 32° N.

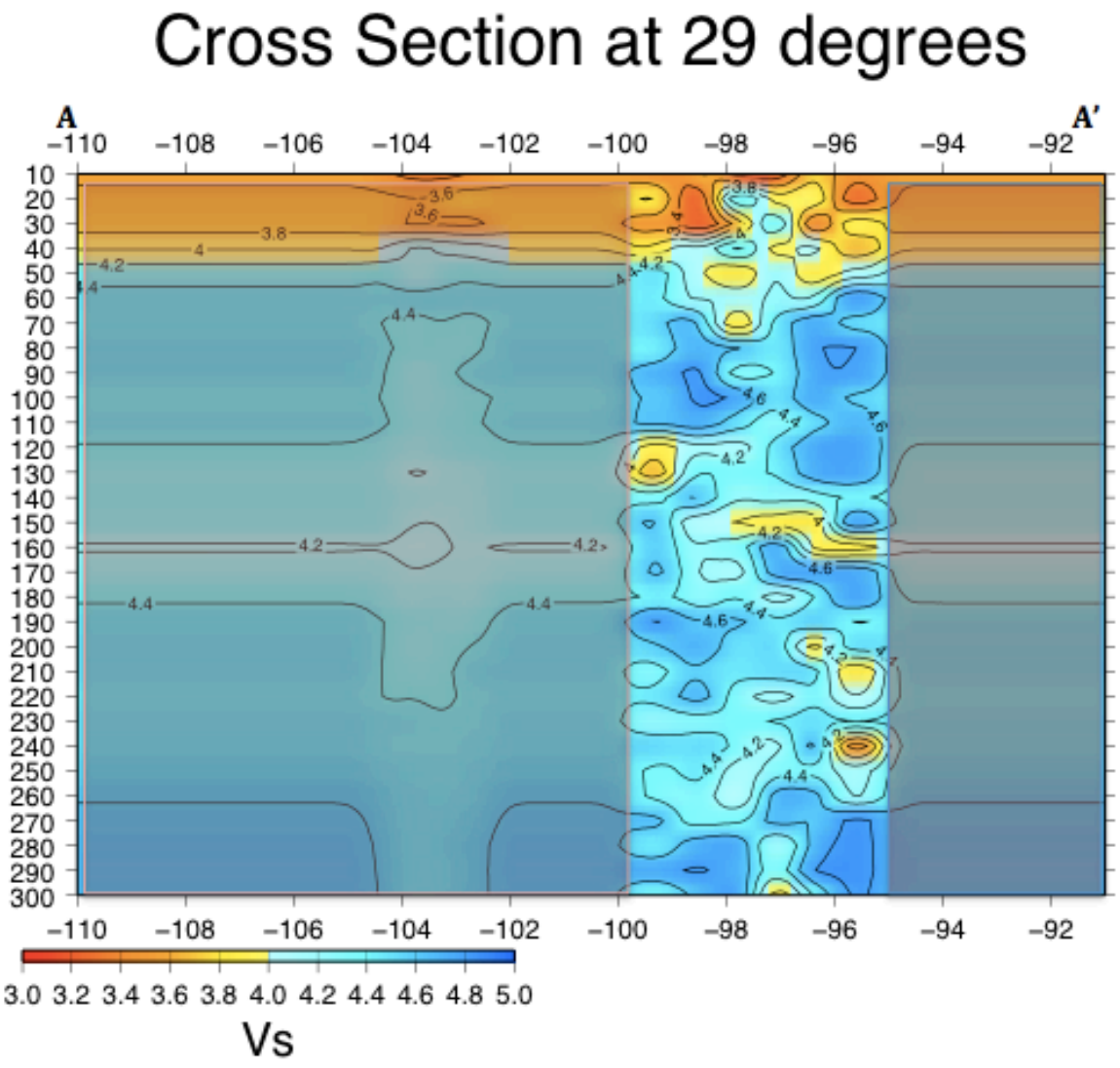

Figure 7.4: Cross Section at 29^0 N latitude showing shear wave velocity in km/s. Shaded region shows lack of data and stations. A-A' denotes cross section on depth slice Figure 14.

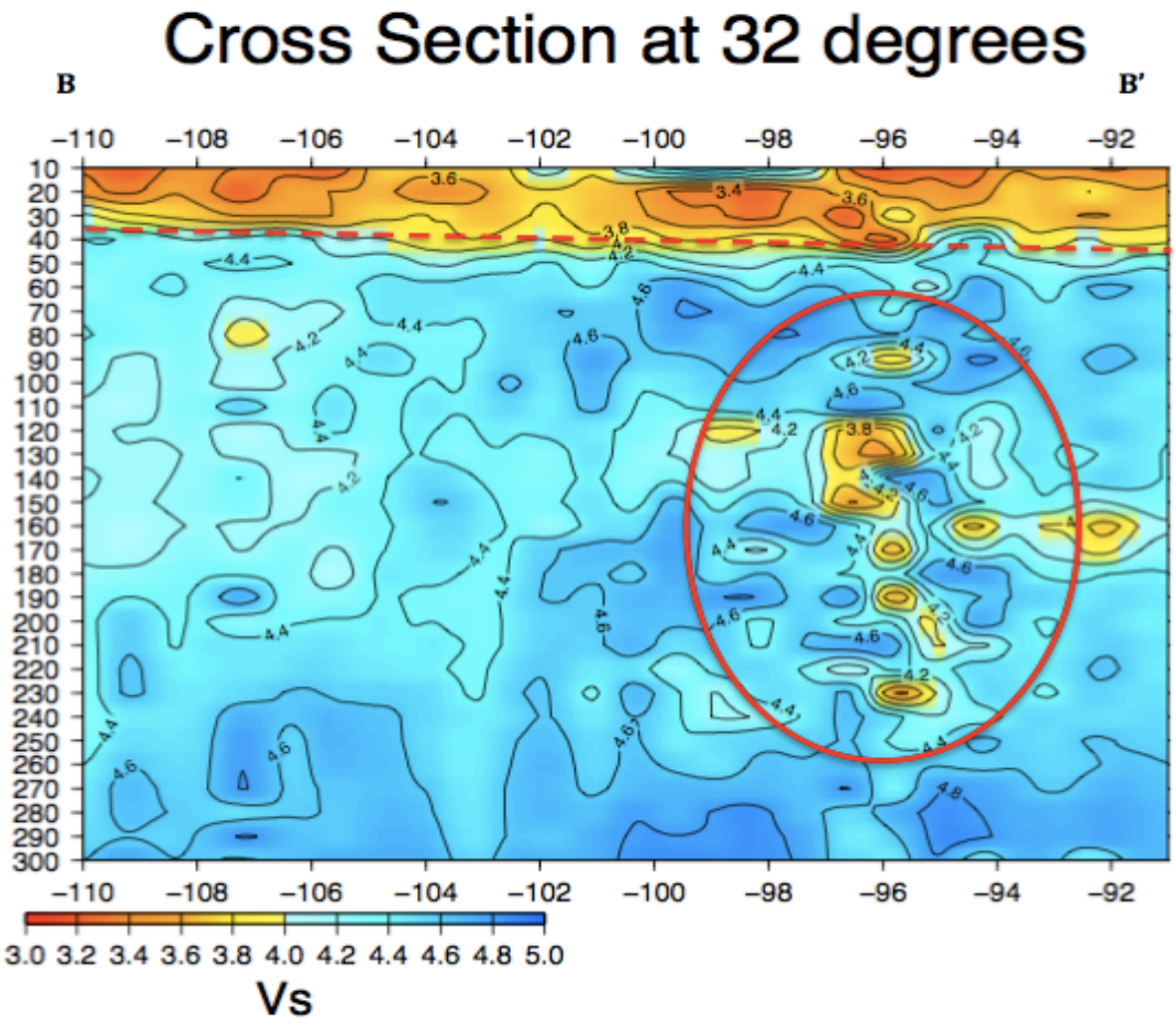

Figure 7.5: Cross Section at 32^0 N latitude showing shear wave velocity in km/s. Cross Section covers largest W-E line across Texas into Louisiana. Low velocity anomalies extend from approximately 60 – 230 km depth. B-B' denotes cross section on depth slice Figure 14. Moho discontinuity denoted by dotted red line.

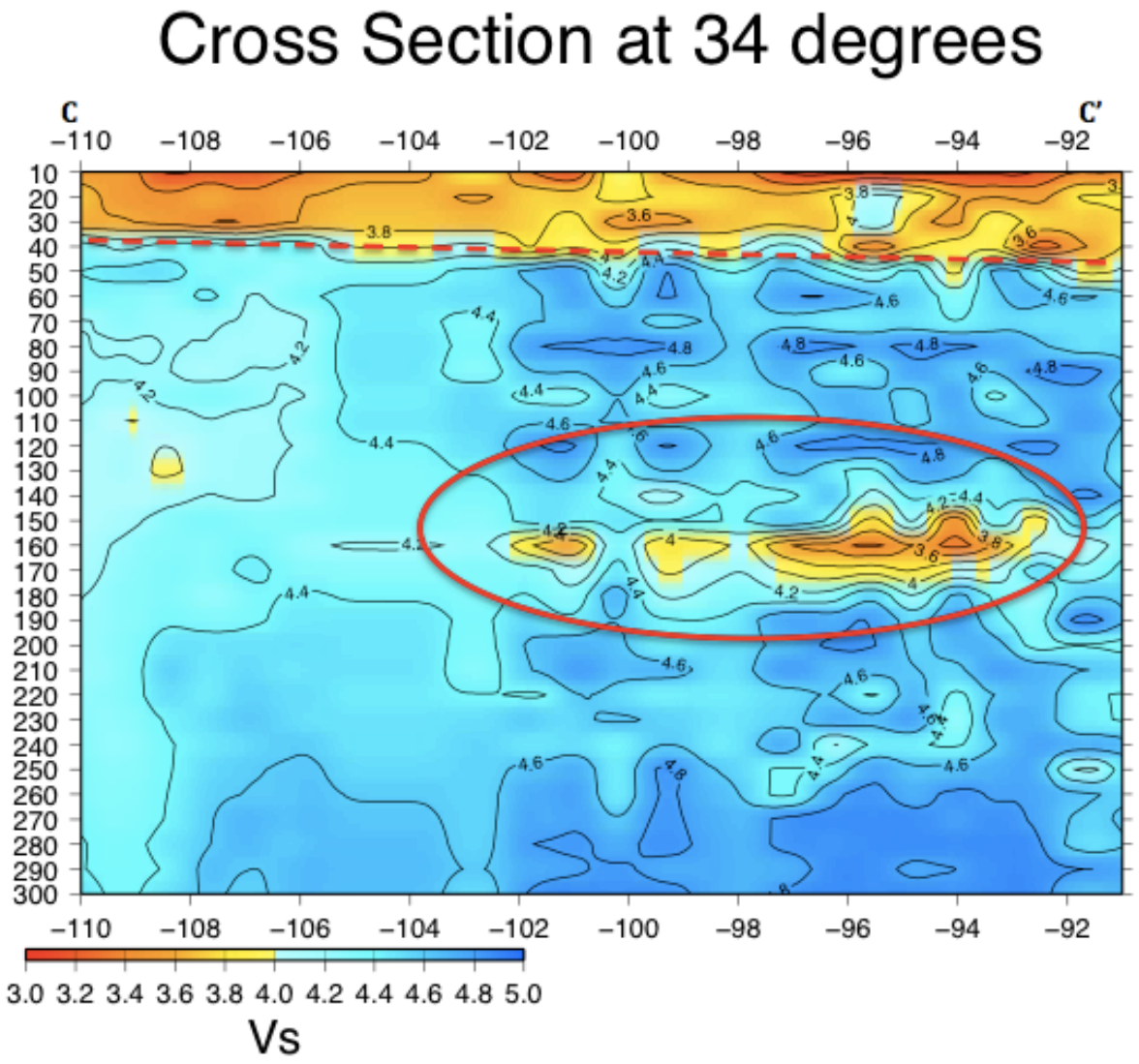

Figure 7.6: Cross Section at 34^0 N latitude showing shear wave velocity in km/s. Cross Section covers New Mexico, Texas, southern Oklahoma, and Arkansas W-E. Low Vs anomalies appear at 160km depth. C-C' denotes cross section on Figure 14. Moho discontinuity denoted by dotted red line.

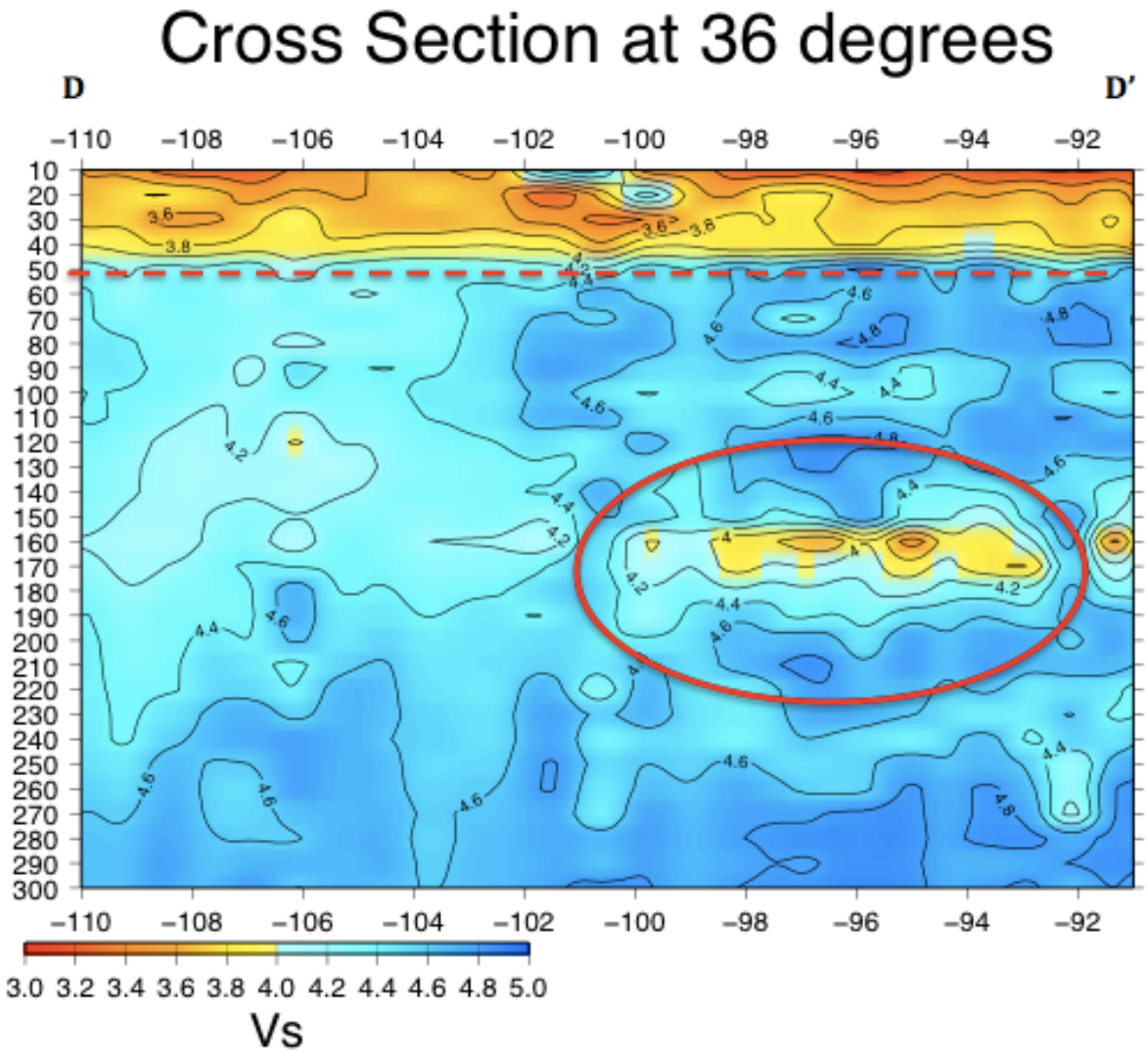

Figure 7.7: Cross Section at 36^0 N latitude showing shear wave velocity in km/s. Cross Section covers New Mexico, Texas panhandle, northern Oklahoma, and northern Arkansas W-E. Low Vs anomalies appear at 160km depth. D-D' denotes cross section on Figure 14. Moho discontinuity denoted by dotted line.

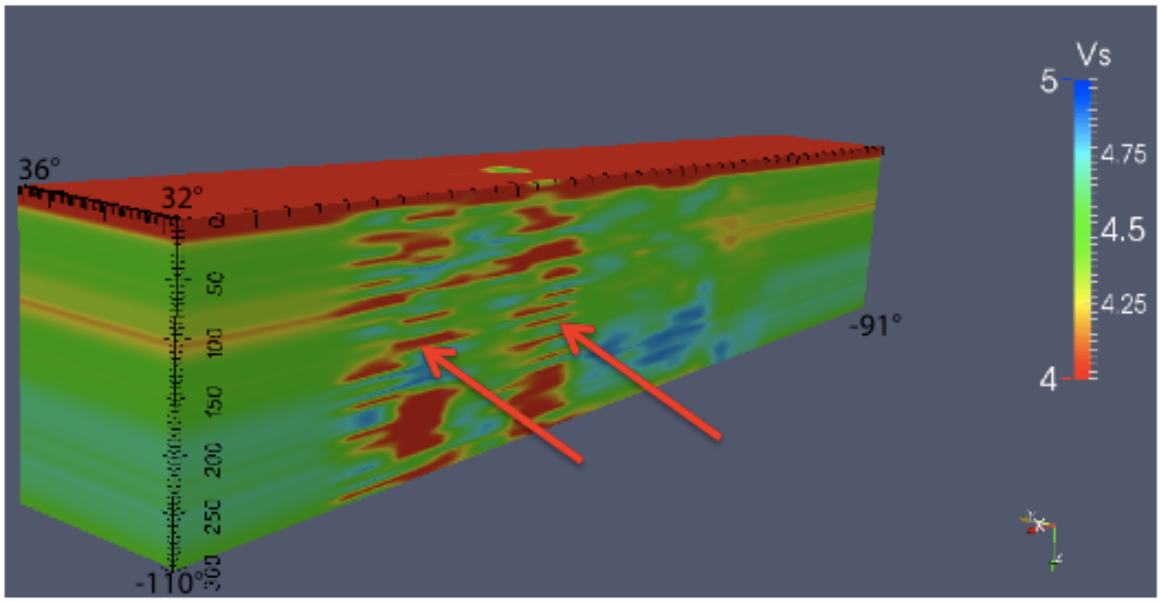

Figure 7.8: 3-D S-Wave velocity model showing shear wave velocity in km/s. Low velocity anomalies present at approximately -106^{0}W to -95^{0}W longitude. Arrows point to possible ringing due to noise or bad data.

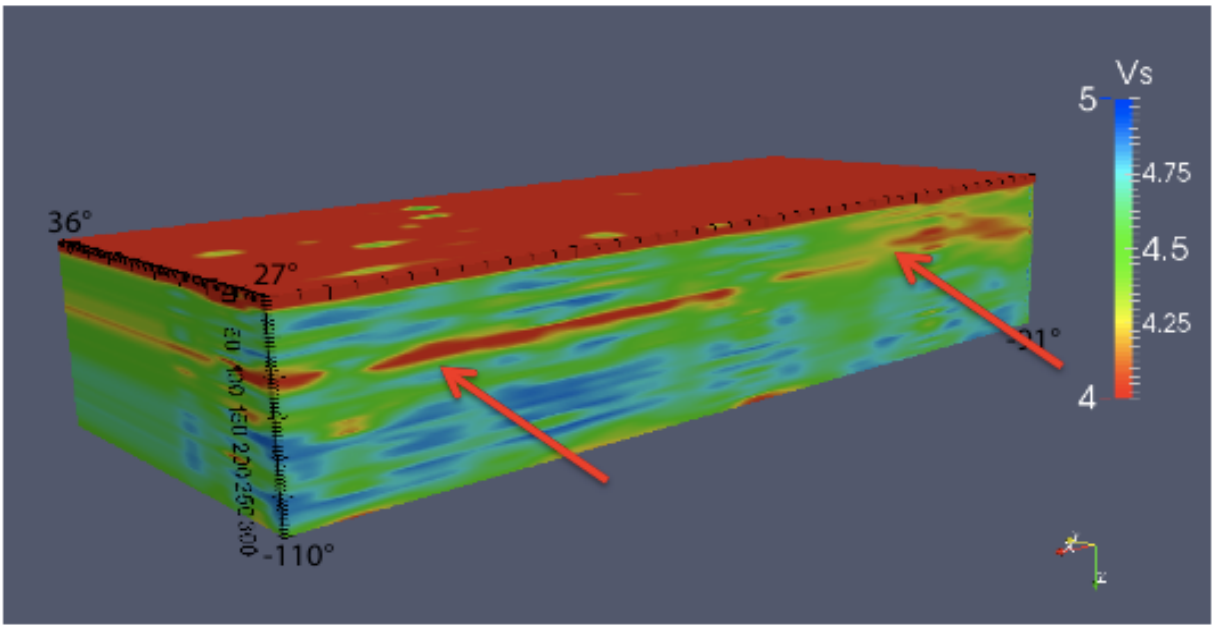

Figure 7.9: 3-D S-Wave velocity model showing shear wave velocity in km/s. Model extends to 27^0N latitude to the south. Low velocity anomalies present at approximately -106^0W to -95^0W longitude shown by red arrows.

Chapter 8: Discussion

I use a PDIP joint inversion of receiver functions and surface wave group dispersion data to create 1- D s-wave velocity models of the earths subsurface along New Mexico, Texas, Oklahoma, Arkansas and Louisiana. The 1-D velocity profiles are interpolated to 3-D models. I focus solely on this region, which leads to differences from previous studies that focus on a much smaller region (Sosa et al., 2013). This study shows features relevant to the evolution of rifting in the study region.

Results are shown in Figures 7.1-7.9. The 1-D velocity profiles of the study area show the upper mantle velocity structure down to 300 kilometers depth. Figure 7.4 shows inconsistent results due to lack of data (stations) in the shaded regions of the cross section map at 29^0 N latitude. This is due to the fact that there is no station coverage from approximately -110^0 W to -100^0 W and from -95^0 W to -91^0 W at the cross section along 29^0N latitude. Velocity model shown in figures 7.6 and 7.7 show S-Wave velocity anomalies at approximately 160 kilometers depth that may be attributed to the transition of the Lithosphere-Asthenosphere Boundary (LAB). The nature of the LAB boundary determines the mechanical and compositional coupling between rigid plates and the conveying mantle. Previous seismic tomographic studies suggests that the LAB is not determined by a purely thermal model, but rather it is affected by the presence of partial melt material in the asthenosphere. Evidence from converted seismic phases indicates a sharp decrease in shear wave velocity 90–110 km below continental crust (Rychert et al., 2005). This is consistent with the low velocity findings in this study shown in Figure 7.7.

The Moho discontinuity can clearly be seen in cross section figures 7.5-7.7 at approximately 30-40 kilometers depth displayed by a sharp velocity contrast. Figures 7.8-7.9 show distinct S-Wave velocities at approximately 30-40 kilometers depth, which coincide with

previous crustal thickness studies where the crust averages a thickness of 35 kilometers in the same region (Irie 2011). Figure 7.6 shows distinct S-Wave velocity anomalies beginning at 80 kilometers and extending to approximately 230 kilometers deep. Previous crustal thickness studies (Sosa et al.,) show a thinner crust at 96^0 W quite possibly producing those low velocity anomalies, possibly indicating a heat source underneath the stations in that region that can be seen in 3-D model figure 7.9.

Figure 7.1 is key because it provides insight into the Brittle-Ductile transition zone (BDT). The map view depth image shows velocity variations; particularly higher shear wave velocities in northern Arkansas, Oklahoma and the Texas coastline. The brittle-ductile transition zone is approximately 13-18 kilometers deep, at this depth rock becomes less likely to fracture, and more likely to deform ductilely by creep. This happens because the confining pressure increases the brittle strength of a material, simultaneously the ductile strength of a material decreases with increasing temperature. This increase in strength within the crust may be indicated by the higher velocity anomalies in figure 7.1. The Moho region is shown in figure 7.2 at 40 kilometers depth. Figure 7.2 also shows high velocity anomalies along the Texas coast and in the Rio Grande Rift indicating a seismically fast mantle underlies these regions. The depth slice at 160 kilometers depth (Figure 7.4) depicts the LAB. Cross section 32^0 N (Figure 7.6) shows velocity anomalies that coincide with 3-D velocity model (Figure 7.9) and previous studies possibly indicating a mantle plume or increased water content leading to silicate melt and increased temperatures (Mierdel 2007). Deep mantle welling cannot be seen which leads to the conclusion that the mechanism for rift formation remains ambiguous. Future work must include other data sets that show to be compatible such as gravity, magnetic, and travel times data.

Chapter 9: Conclusion

This study presents a new model of crustal and upper mantle velocities that covers a large geographical region in the southwest United States. This study extends the previous work done by Sosa et al. (2014) in the Rio Grande Rift into the states of Texas, Oklahoma, Louisiana, and Arkansas. The models coincide with previous models in recent studies as we can see active rift zones in the region of the Rio Grande rift but cannot make the same determination for the rest of the states. The resulting models show low velocity regions at the Moho and LAB but do not present clear evidence of a possible deep mantle plume that would drive any active rifting in the study region. Further data collection in sparse regions such as the states of Chihuahua and Coahuila can enhance the accuracy of our velocity models. The implementation of more geophysical data sets into our inversion, such as gravity and travel times can better constrain geological structures and increase resolution of the velocity models.

References

Adams, D.C. and Keller, G.R, 1993, possible extension of the Midconinent Rift in west Texas and eastern New Mexico, Canadian Journal of Earth Sciences, 31, 709-721.

Ammon, C.J., 1991, The Isolation of Receiver Effects From Teleseismic P Wave forms, Bull. Seism. Soc. Am. 81, 2504-2510

Corner, B., Cartwright, J., and Stewart, R., 2002, Volcanic passive margin of Namibia: Apotential fields perspective, in Menzies, M.A., Volcanic Rifted Margins: Geological Society of America Special Paper362, 203-220.

Colombo D., and De Stefano M., 2007, Geophysical modeling via simultaneous joint inversion of seismic, gravity, and electromagnetic data: Application to prestack depth imaging: The Leading Edge, 26**,** 326-331.

Dickinson W.R., Gehrels G.G., 2008, U-Pb ages of detrital zircons in relation to paleogeography: Triassic paleodrainage networks and sediment dispersal across southwest Laurentia: Journal of Sedimentary Research, v. 78, p. 745– 764.

Dickinson W.R., Lawton T.F., 2001, Tectonic setting and sandstone petrofacies of the Bisbee basin (USA-Mexico): Journal of South American Earth Sciences, v. 14, p. 475– 504, doi: 10.1016/S0895-9811(01)00046-3.

Julia, J., Ammon, C.J., Herrmann, R.B., and Correig, A.M., 2000, Joint inversion of receiver function and surface wave dispersion observations, Geophys. J. Int., 143, 1-19.

Lawton T.F., McMillan N.J., 1999, Arc abandonment as a cause for passive continental rifting: Comparison of the Jurassic Mexican Borderland rift and the Cenozoic Rio Grande rift: Geology, v. 27, p. 779– 782, doi: 10.1130/0091-7613(1999)027<0779:AAAACF>2.3.CO;2.

Liu, K., Levander, A., Niu, F., Miller, M. S., 2011, Imaging crustal and upper mantle structure beneath the Colorado Plateau using finite-frequency Rayleigh wave tomography. Geochemistry, Geophysics, Geosystems. Vol. 12 (7), pp. doi:10.1029/2011GC003611.

Mickus, K., Stern, R.J., Keller, G.R. and Anthony, E. Y., 2009, Potential field evidence for volcanic rifted margin along the Texas Gulf Coast, Geology, Vol 37, No.5, 387-390.

"Observatories." *EarthScope: An Earth Science Program*. N.p., n.d. Web. 26 Nov. 2013.

Shultz, C., Myers, S., Hipp, J., Young, C., 1998, Nonstationary Bayesian kriging: A Predictive Technique to Generate Corrections for Detection, Location, and Discrimination, *Bull.Seismol. Soc. Am.,* 88**,** 1275-1288.

Sosa, A., Velasco, A., Velasquez, L., Argaez, M., Romero, R., 2013, Constrained optimization framework for joint inversion of geophysical data sets. Geophysical Journal International 195:3, 1745-1762

Zhang, H., Turber,C.H., 2003 Double-difference tomography: the method and its application to the Hayward Fault, California. Bull. seism. Soc. Am.,93:1875-1889.

Vita

Sergio H. Celis was born in Ciudad Juarez, Chihuahua, Mexico the first of two children of Sergio and Maria Celis. After graduating from Burges High School in El Paso, Sergio enrolled at The University of Texas at El Paso as a mechanical engineer major. He changed his major to Geophysics and graduated with a Bachelor of Sciences in Geophysics in May of 2012. He worked as a research assistant for Dr. Aaron A. Velasco during his undergraduate studies and took part in the dynamic earthquake triggering research working with graduate students. He also worked as a research assistant for Dr. Rhaed Aldouri in the Utep Geospatial center from December 2010 to May 2012. In August 2012 he was accepted into the Geophysics graduate program and studied under Dr. Aaron A. Velasco. Sergio presented his graduate research work at the American Geophysical Union meeting in Cancun, Mexico in May 2013. He then presented his graduate research work at the American Geophysical Union meeting in San Francisco in December 2013. Sergio worked as a Geophysics intern at Lewis Energy Oil and Gas Company in the summer of 2014. He graduated from the University of Texas at El Paso with his Master of Science degree in December 2014. He currently works as a Geoscientist at HGI Hydrogeophysics in Tucson, Arizona.

Contact information: shcelis@miners.utep.edu

This thesis/dissertation was typed by Sergio H. Celis